Available online at www.sciencedirect.com

ScienceDirect

Procedia CIRP 74 (2018) 407–412

www.elsevier.com/locate/procedia

10th CIRP Conference on Photonic Technologies [LANE 2018]

Laser drilling of micro-holes in single crystal silicon, indium phosphide and indium antimonide using a continuous wave (CW) 1070 nm fibre laser with millisecond pulse widths

Jessica O. Maclean[a,*], C. Tangkijcharoenchai[b], Stuart Coomber[c], Katy T. Voisey[b]

[a]*School of Physics and Astronomy, University of Nottingham, University Park, Nottingham, NG7 2RD, UK*
[b]*Faculty of Engineering, University of Nottingham, University Park, Nottingham, NG7 2RD, UK*
[c]*Wafer Technology Ltd., 34 Maryland Rd., Tongwell, Milton Keynes, Buckinghamshire, MK15 8HJ, UK*

* Corresponding author. Tel. +44-115-846-6008; fax: +44-115-951-5180. *E-mail address:* Jessica.Maclean@nottingham.ac.uk

Abstract

The laser micro-drilling of "thru" holes, also known as via holes, in Si, InP and InSb semiconductor wafers was studied using millisecond pulse lengths from an IPG Laser Model YLR-2000 CW multimode 2 kW Ytterbium Fibre Laser and a JK400 (400 W) fibre laser, both with 1070 nm wavelength. The flexibility of this laser wavelength and simple pulsing scheme were demonstrated for semiconductor substrates of narrow (InSb E_g 0.17 eV) and wide (InP E_g 1.35 eV)) room-temperature bandgap, E_g, with respect to the photon energy of 1.1 eV. Optical microscopy and cross-sectional analysis were used to quantify hole dimensions and the distribution of recast material for all wafers and, for silicon, any microcracking for both (100) and (111) single crystal surface Si wafer orientations. It was found that the thermal diffusivity was not a sufficient parameter for predicting the relative hole sizes for the Si, InP and InSb single crystal semiconductors studied. Detailed observations for Si showed that, between the threshold energies for surface melting and the irradiance for drilling a "thru" hole from the front surface to rear surface, there was a range of irradiances for which micro-cracking occurred near the hole circumference. The directionality and lengths of these microcracks were studied for the (100) and (111) orientations and possible mechanisms for formation were discussed, including the Griffith criterion for microcracks and the failure mechanism of fatigue usually applied to welding of metals. For Si, above the irradiance for formation of a thru-hole, few cracks were observed. Future work will compare similar observations and measurements in other narrow- and wide-bandgap semiconductor wafer substrates. We demonstrated one application of this laser micro-drilling process for the micro-fabrication of a thru hole precisely-located in the centre of a silicon-based atom chip which had been patterned using semiconductor lithographic techniques. The end-user application was a source of magneto-optically trapped (MOT) cold atoms of Rubidium (^{87}Rb) for portable quantum sensing.

Peer-review under responsibility of the Bayerisches Laserzentrum GmbH.

Keywords: Fibre laser; Ytterbium fibre laser; silicon; Si; InP; InSb; semiconductor material; semiconductor wafer; laser drilling; laser micro-drilling; microcrack; pulse; Griffith criterion; via hole; thru hole; cold atoms; atom chip; magneto-optical trap; MOT

1. Introduction

The interaction of high intensity, short laser pulses was studied for material removal from semiconductor substrates. The laser micro-drilling of Si single crystal wafer substrates was investigated using a single near-infrared (NIR) laser wavelength near 1070 nm using an IPG laser of beam waist diameter (w) 192 µm at the substrate surface and a JK400 laser of w 50 µm. Previous work using the IPG laser demonstrated that a single pulse of milliseconds duration drilled thru-holes of dimensions typically in the range of 200 to 500 µm diameter in materials of bandgap ranging from 1.43 eV (GaAs) to 8.9 eV (sapphire) [1]. This work extended the results of hole micro-fabrication and characterisation to indium phosphide (InP) and indium antimonide (InSb) III-V semiconductor substrates, and also used the JK400 laser,

Peer-review under responsibility of the Bayerisches Laserzentrum GmbH.
10.1016/j.procir.2018.08.158

which has higher irradiance. All semiconductor substrate materials were high quality single crystal wafer substrates suitable for epitaxial growth with a polished front surface of roughness of 2 nm and a wafer thickness in the range of 300 μm to 500 μm.

Under low optical intensities, photons of energies exceeding the semiconductor bandgap are absorbed; it is also known that interfaces lead to scattering and absorption, making some nominally transparent materials opaque, and hence the successful long-wavelength laser drilling of Al_2O_3 [2, 3]. For single crystal semiconductor wafers, the sub-bandgap absorption results from reduction of the bandgap due to surface melting by high optical intensity [4], the presence of impurities or structural imperfections, as well as some absorption being attributable to free carriers generated by the absorbed photons [5]. Wafer substrates were commercially-sourced "epi-ready" process trial semiconductor substrate wafers of 50 mm diameter, some of which were manufactured at Wafer Technology Ltd., UK of typical root-mean-square surface roughness, R_{rms}, 2 nm on the epi-ready side and R_{rms} 2 μm on the rear side. Previous work demonstrated the importance of surface roughness in the entrance hole dimension and compared the difference between the entrance and exit diameters of holes for different substrate materials (sapphire, gallium arsenide, silicon) also using a wavelength of 1070 nm and the IPG laser of irradiance in the range of ($1.7x10^6$ - $1.1 x10^7$) W cm^{-2} [1]. We describe here the overall results for the laser drilling of Si, InP and InSb in terms of hole dimension achieved (Fig. 1). A dependence of micro-cracking on irradiance was identified for Si.

Nomenclature

w	Beam waist diameter
E	Energy required for melting and vaporisation (J)
m	Mass of material removed (kg)
ΔT	Temperature change (K)
C_p	Specific Heat Capacity at constant pressure ($Jkg^{-1}K^{-1}$)
L_v	Latent heat of vaporisation (Jkg^{-1})
L_m	Latent heat of melting (Jkg^{-1})
E_1	Threshold energy for piercing the surface
E_2	Threshold energy for a "thru" hole
E_g	Room temperature bandgap

2. Method

The lasers used were multimode Yb fiber laser (IPG YLR-2000) with 1070 nm wavelength, a maximum power of 2 kW and w of 192 μm. For a subset of the results, a different Yb fiber laser, (GSI JK400FL) of 400 W maximum power with focus diameter 50 μm was used, enabling smaller hole sizes to be achieved. Both lasers had a minimum pulse length of 1 ms. The principal drilling parameters (power, pulse length, focal position, wafer orientation) were varied to achieve holes of a range of dimensions through single crystal Si (E_g 1.1 eV), InSb (E_g 0.17 eV) and InP (E_g 1.35 eV) using the 1070 nm wavelength and a minimum pulse length of 1 ms (see Figs. 1(a.) and 1(b.)). Substrates were placed with the highly-polished face a few degrees from the normal to the laser beam which was focused on the substrate surface. Samples were mounted a few cm above the translation stage resting on a ring-shaped ledge of a precision-machined, stainless steel cylindrical holder. An assist gas of Ar was used in all experiments, at a flow pressure between 0.5 and 2 bar, emerging concentric with the laser beam at a distance of 1 mm from the wafer surface. This directed material ejected away from the front surface of the hole, reducing spatter around the hole. We focus here on the presentation of our results of micro-holes in silicon following the analysis of hundreds of holes, laser-drilled under different parameters. Optical microscopy was carried out using a Nikon Eclipse LV100ND or an Olympus MX51 for the assessment of hole dimensions and hole shape (Fig. 3), crack lengths and directions, and recast material location. the reproducibility of the hole dimension and any micro-cracking resulting from mechanical stress [6]. Having investigated the robustness for larger diameter holes, we demonstrated our first application to an atom chip designed for a source of ultra-cold atoms in a portable quantum sensor. The micro-hole was an aperture for optical access and was an orifice for differential pumping under UHV conditions (Fig. 4). No further process steps were required for the hole other than solvent cleaning. Subsequent evaluation of this laser drilling process in terms of a device reliability assessment would be dependent on the application. For example, in an application of a via hole to solar cell devices, as an "emitter wrap thru" contact, an assessment of open circuit voltage as a function of perimeter to area ratio for various via dimensions and areal densities would be important for a solar cell device [7] and efficiency improvements of >2% have been demonstrated for plasma-etched and wet-chemically-passivated via architectures for high concentration multi-junction solar cells as compared with standard top contacts [8].

A simple calculation, based on data in Table 1, predicting E (J), the energy required for melting and vapourisation which is the energy required to remove a typical cylindrical volume of the single crystal silicon of diameter 250 μm in terms of melting followed by vapourisation, suggests that a single pulse of 1 ms at the maximum (peak) power of 2 kW of energy 2 J should exceed the energy required by a factor of 8;

$$E\ (J) = m\ (Cp\ \Delta T + Lm + Lv) \quad (1)$$

The corresponding energies for InSb and InP are 0.186 mJ and 0.139 mJ. This simple model does not account for the thermal diffusivity of the materials and the extent of the area affected by rapid surface heating. There is the potential for a brittle material to crack as the result of rapid differential thermal expansion and contraction. The Griffith criterion predicts that a crack will propagate when a tensile stress is applied if the crack propagation results in a decrease in elastic strain energy which exceeds the increase in surface energy due to the surface area of the crack [6]. Using Equation 1 the pulse energy exceeds the energy required by InSb by a factor of 11 and for InP by a factor of 14.

Table 1. Thermodynamic parameters and material properties of single crystal Si used to estimate the energy required to drill a microhole of 250 µm diameter by melt-ejection.

Material Property	Data for Si
Bandgap at 300 K, E_g	1.12 eV
Specific heat capacity, Cp	712 J/Kkg
Latent heat of vaporization, L_v	1926 kJ/kg
Latent heat of melting, L_m	1.42×10^6 J/kg
Melting point, T_m	1410°C
Density, □	2330 kg/m^3
Energy requirement, E (J) (estimated from Equation (1))	249 mJ
Laser pulse energy at maximum power, P	2 J

3. Results

Figs. 1(a.) and 1(b.) show data for the diameter, in microns, of the entrance and exit holes as a function of total pulse energy for holes drilled in silicon wafers, using the 2 different lasers. The total pulse energy was in the range from 0.5 J (500 W for 1 ms) to 20 J (2000 W for 10 ms). The irradiance of the JK400 laser was ($4x10^6$ – 1.6 x 10^7) Wcm^{-2} whereas the irradiance of the IPG laser was (1.4-5.4) x 10^6 Wcm^{-2}. When using the JK400 laser, which has the higher irradiance and focal diameter of 50 µm, and 10 ms pulse duration, at lower energies of (1.5-2) J, the hole dimensions exceeded the focal diameter and depended strongly on total pulse energy. A decrease in hole dimension with increase in energy from 200 µm to 160 µm was observed as the energy changed from 1 J to 3 J. Above 2.3 J pulse energy the hole was cylindrical. This suggested that there was efficient absorption of the 1070 nm wavelength and that the melt-ejection mechanism removed silicon quickly at high energies and a short time for thermal diffusivity to affect the hole dimension. In the case of the IPG laser (Fig. 1(b.)), which has the lower irradiance and focal diameter of 192 µm, large total pulse energies exceeding 4 J resulted in a ratio of the entrance to exit diameter in the range (1.3-1.4) with the entrance diameter having a value around 350 µm and an exit around 250 µm. Overall, it may be seen from Figs. 1(a) and 1(b.) that a wide range of hole dimensions was achieved in Si.

Figs. 2(a.) and 2(b.) show the IPG laser results for InP and InSb, using a 10 ms pulse for InP and both 1 ms and 10 ms pulses for InSb. For pulse energies in the range of (5-15) J for InP, the hole dimensions and ratio were similar to those of silicon, the dimensions achieved for the entrance diameter being (0.8-0.9) those of silicon. The initial absorption may be lower until surface melting occurs because of the wider bandgap. For a single 10 ms pulse, InP showed increasing entrance and exit hole sizes with increasing pulse energy, the entrance and exit being most similar in dimension with a pulse energy of 10 J. The range of entrance diameters achieved were 250 to 320 µm. In contrast, thru-holes were drilled in InSb at very low pulse energies (< 1 J) and increase of pulse energy strongly increased the hole diameter.

1(a.)

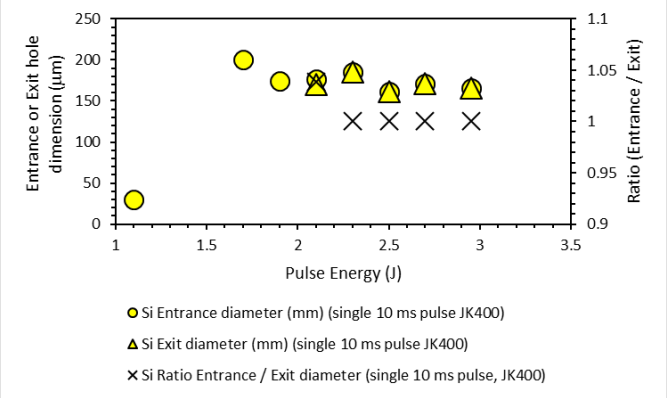

1(b.)

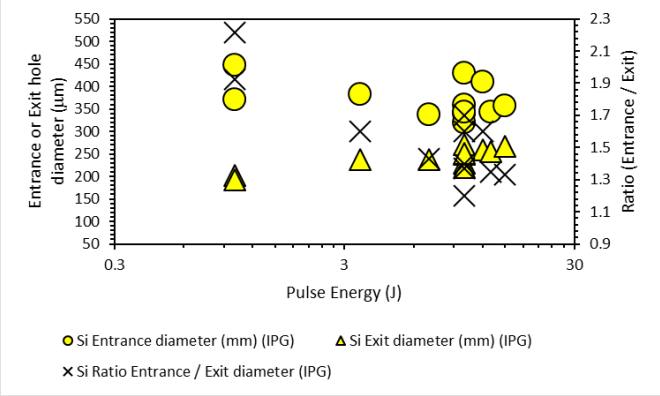

Fig. 1. (a) Microhole dimensions in µm for holes drilled in Silicon using a single 1 ms pulse and the JK400 laser. The lowest energy datapoint corresponds to an incomplete hole; (b) Microhole dimensions in µm for holes drilled in Silicon using a single 1 ms or 10 ms pulse and the IPG laser.

A comprehensive study of InSb revealed a wide range of dimensions were accessible with this wavelength and pulse energy range, from (100–650) µm, and the cross-sections of the holes could be either positively or negatively tapered depending on the pulse energy. This was consistent with the high absorption of the narrow bandgap material to this 1070 nm wavelength. It is notable that the relative thermal diffusivities of the 3 semiconductors (Si 8.8 x 10^{-5} m^{2}s^{-1}, InP 3.72 x 10^{-5} m^{2}s^{-1} and InSb 1.6 x 10^{-5} m^{2}s^{-1} [9]) do not predict simply the relative hole dimensions. Precise control of pulse energy and surface quality is therefore required for narrow bandgap materials when using this wavelength. We previously demonstrated the importance of surface roughness in the control of hole dimension for silicon, demonstrating that the ratio of entrance to exit diameters was dependent on the front surface polish specification [1].

2(a.)

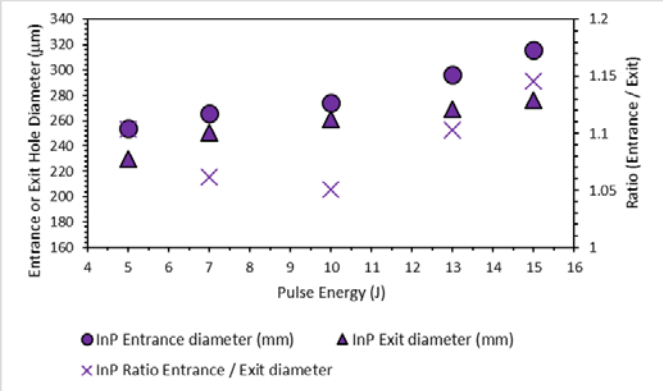

2(b.)

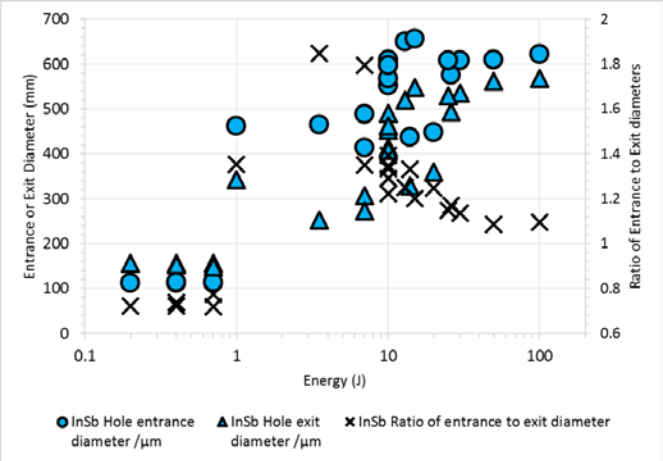

Fig. 2. (a) Microhole dimensions in µm for holes drilled in Indium Phosphide using a single 10 ms pulse and the IPG laser. Each datapoint shows the mean of a set of 9 identical holes for each parameter set; (b) Microhole dimensions in µm for holes drilled in Indium Antimonide using a single 1 ms and 10 ms pulses and the IPG laser. Each datapoint shows the mean of a set of 5 identical holes for each parameter set.

A previous study [10] of the microstructure at low pulse energies examined the entrance hole dimensions as a function of laser power for a single 1 ms pulse when using the full 2 kW output of the IPG laser. At the threshold for surface melting the hole was circular and then became elliptical until it was circular again when a thru-hole was made. This ellipticity may be the origin of the microcracking observed at intermediate energies. Figs. 3(a.), (b.) and (c.) shows plan-view images of holes of approximately 300 µm in diameter laser-drilled in Silicon (100). The morphology of the hole evolved as a function of power showing the effects of melting, vapourisation and re-solidification. At the threshold for surface melting, E_1, the re-solidified hole exhibited morphology similar to that of the Marangoni effect. A novel application of the laser-drilling technique was demonstrated for quantum technologies research [11]. The compatibility of the laser-micro-drilling technique with semiconductor wafer nanofabrication techniques used for the components of a cold atom quantum sensor was demonstrated. A hole was precisely located in a silicon wafer which had already been patterned and dry-etched with a diffraction grating designed for 780 nm laser light and trapping of ultra-cold atoms of Rb a few mm above its surface [12].

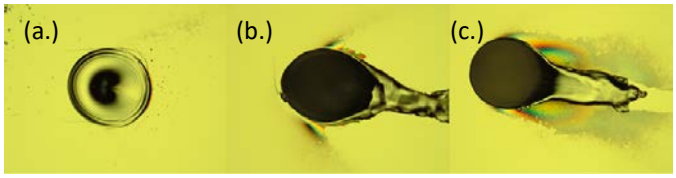

Fig. 3. Optical microscopy showing the threshold energy of 0.5 J for laser micro-drilling an epitaxial Si(100) wafer for a 1 ms pulse at 1070 nm wavelength and exhibiting concentric ripples, possibly similar to the Marangoni effect and associated micro-cracking following the principal crystallographic directions (left - 500 W (a.), centre - 700 W (b.), right - 1000 W (c.)). Holes were approximately 300 µm in diameter. No sample cleaning was performed post-drilling.

Fig. 4 shows a photographic image of a whole patterned silicon wafer with a central laser-drilled hole using the IPG laser. The hole which was located in the centre of the pattern using a precision translation stage underneath the laser-drilling beam. The hole diameter was 550 µm and the exit diameter was 450 µm. The subsequent successful achievement, under vacuum conditions, of a cloud of magneto-optically trapped Rubidium cold atoms a few mm above the hole demonstrated that the presence of the hole did not adversely affect the optical trapping. This also confirmed that spattered material was successfully removed from the patterned surface by standard solvent cleaning techniques.

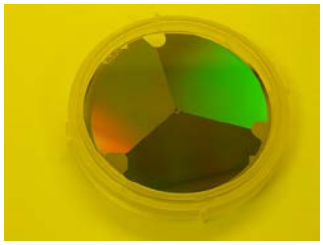

Fig. 4. (a) Hole of approximately 550 µm diameter laser-micro-drilled in the centre of a patterned silicon wafer (used as an atom chip for producing magneto-optically-trapped Rb atoms by diffraction of a 780 nm laser beam) by drilling a single hole at 1400 W for 2 ms and a *w* of 400 µm. The hole was approximately circular and exhibited relatively short length of cracks approximately parallel to, and originating from, the hole circumference.

Two different and technologically important wafer orientations of silicon, (100) and (111), were compared in terms of the total crack length as a function of power and the hole dimensions achieved [10]. The entrance and exit hole diameters were measured at 3 irradiances (400 W or 1.4×10^7 Jm^{-2}, 700 W or 2.4×10^7 Jm^{-2}, 1000 W or 3.5×10^7 Jm^{-2}) as were the total crack lengths. The drilling threshold corresponded to 0.4 J of energy for both wafer orientations. An intermediate range of irradiance was identified, between the onset of drilling (E_1) and the achievement of a thru-hole (E_2), which exhibited micro-cracking. In this intermediate region the dimension of the hole increased as a function of power and then the dimension tended to reach a plateau. The results [10] demonstrated the similar behaviour of the melt threshold and thru-hole thresholds for the (100) and (111) wafer orientations of silicon and showed similar hole dimensions and tended to a

plateau in dimension at high power suggesting that the leading edge of the pulse determined the melt-ejected volume and that the diameter did not evolve during the duration of 1 ms. The intermediate region in which many cracks were generated may correspond to a regime in which the temperature gradient causes the tensile strength to be exceeded and fracture occurs. Measurements above E_2 showed a weak variation in hole dimension and indicated that micro-cracking was a gradually increasing function of pulse energy, increasing at a rate of about 50 μm J^{-1}. The melt-ejection mechanism expels material by the pressure of a vapourised gaseous plasma exiting the hole and this mechanism was observed for all laser drilling parameters used in this study. The computational modelling of these physical processes was reported by Verhoeven [13]. This contrasts with the proposed mechanism of Yu [4] in which a similar wavelength to 1070 nm was used to remove silicon using femtosecond pulses in an ablation process which relied on maintaining a thermal equilibrium between thermal diffusion and incident optical energy, to provide a high temperature gradient at the melted surface. The microcracking of silicon between E_1 and E_2 may be analogous to the fatigue failure seen in the welding of metals [14]. Cyclic loading of welds subjects the weld to an oscillating stress over time, resulting in both tensile and compressive forces causing the metal surface to exhibit intrusions and extrusions along slip planes. Our results, achieving a wide range of hole dimensions, demonstrate both the control of hole dimension and the minimisation of associated micro-cracking. Melted material remaining at the hole entrance may play some role in reducing crack initiation.

4. Conclusions

The ability to rapidly drill through hundreds of microns of material in order to create and locate a hole of sub-mm dimensions precisely, in a brittle substrate, such as a semiconductor wafer, is a novel capability. A fibre laser of wavelength 1070 nm was used with maximum power 2 kW and beam diameter, *w*, 192 μm, or, alternatively, a 400 W Yb fibre laser of beam diameter 50 μm. Holes of diameters between 70 μm and 600 μm were achieved in Si. We report for the first time that holes were achieved in both InP (diameters 200-400 μm) and in InSb (hole diameters in the range 100-600 μm) compound semiconductors, having bandgaps both higher and lower respectively than that of the photon energy used. The relative dimensions of the holes was not simply related to the thermal diffusivity of each single crystal semiconductor material. When using the minimum pulse length of 1 ms, the pulse energy thresholds were established for piercing a hole in both (100)- and (111)- oriented silicon. For both crystallographic orientations, observations and measurements were consistent with a simple conceptual model of the presence of micro-cracks around the holes in silicon within a critical irradiance range between the energy threshold for surface melting, E_1, and the energy threshold for drilling of a thru hole, E_2. Therefore the pulse energy for minimal micro-crack length must be selected for brittle materials as a function of the material properties. Future work will investigate the requirements for the epitaxial structure or surface passivation of the hole in order to incorporate this fabrication step into the process flow of a semiconductor device such as a photodetector or solar cell. Importantly, these results demonstrate that elaborate pulsing schemes at UV wavelengths for material ablation are not essential for the production of micro-holes in semiconductor substrates. The holes achieved so far are of sufficient quality for a mechanical aperture (e.g. as a hole of specific vacuum conductance) or in order to provide optical access (e.g. for optical tweezing or trapping of ultracold atoms or ions). The application to an atom chip was demonstrated in this work and may be useful for large grating magneto-optical traps (MOT's) as ultra-cold atom cloud sources for quantum technologies [11]. The 1070 nm wavelength is flexible for laser-drilling in manufacturing processes for a wide range of materials.

Acknowledgements

This work was supported by the Engineering and Physical Sciences Research Council [grant number SM-30535 EP/M013294/1] through the EPSRC UK Quantum Technologies Hub for Sensors and Metrology. J.O. Maclean wishes to thank S. Branston for technical assistance.

References

[1] Maclean J. O., Hodson J. R. and Voisey K. T., Laser Drilling of Via Micro-holes in Single-crystal Semiconductor Substrates using a 1070 nm Fiber Laser with Millisecond Pulse Widths. *Proc. of Society of Photo-Optical Instrumentation Engineers (SPIE)* 9657 (2015) 965704-1-6 doi: 10.1117/12.2175898

[2] Hanon M.M., Akman E., Oztoprak B.G., Gunes M., Taha Z.A., Hajim K.I., Kacar E., Gundogdu O. and Demir A, Experimental and theoretical investigation of the drilling of alumina ceramic using Nd:YAG pulsed laser. *Optics and Laser Technology*, 44(4) (2012) 913-922.

[3] Beyer H., Ross W., Rudolph R., Michaelis A., Uhlenbusch J. and Viol W., Interaction of CO2-laser pulses of microsecond duration with Al_2O_3 ceramic substrates. *J. Applied Physics*, 70(1) (1991) 75-81.

[4] Yu K.X.Z., Wright L. G., Webster P.J.L. and Fraser J. M., Deep Non-linear Ablation of Silicon with a quasi-Continuous wave fiber laser at 1070 nm. *Optics Letters*, 38(11) (2013), 1799-1801.

[5] Ambacher O., Rieger W., Ansmann P., Angerer H., Moustakas T.D. and Stutzman M., Sub-bandgap absorption of gallium nitride by photothermal deflection spectroscopy, *Solid State Communications,* 97(5) (1996), 365-370.

[6] Smallman R.E. and Ngan A.H.W. (Ed.) *Modern Physical Metallurgy 8th Edition,* ISBN: 978-0-08-098204-5 Berlin: Elsevier. 2014.

[7] Ahn S., Huang D.J., Park H.K. and Grigoropoulos C.P., Femtosecond laser drilling of multicrystalline silicon for advanced solar cell fabrication. *Appl. Phys. A* 108 (2012), 113-120.

[8] De Lafontaine, M., Darnon, M., Colin, C., Bouzazi, B., Voltatier, M., Ares, R., Fafard, S., Aimez, V., Jouad, A., Impact of Via Hole Integration on Multijunction Solar Cells for Through Cell Via Contacts *IEEE J. Photovoltaics*, 7(5) 1456-1461 (2017)

[9] http://www.ioffe.ru/SVA/NSM/Semicond/

[10] Maclean J.O., Hodson, J.R., Tangkijcharoenchai, C., Al-Ojaili, S., Rodsavas, S., Coomber, S., Voisey, K.T., Lasers in Engineering, 39(1-2) 53-65 ISSN: 0898-1507 (2018)

[11] K. Bongs, V. Boyer, M.A. Cruise, A. Freise, M. Holynski, J. Hughes, A. Kaushik, Y.-H. Lien, A. Niggebaum, M. Perea-Ortiz, P. Petrov, S. Plant, Y. Singh,A. Stabrawa, D. J. Paul, M. Sorel, D.R.S. Cumming, J.H. Marsh, R.W. Bowtell, M.G. Bason, R.P. Beardsley, R.P. Campion, M.J. Brookes, T. Fernholz, T.M. Fromhold, L. Hackermuller, P. Krüger, X. Li, J. O. Maclean, C.J. Mellor, S.V. Novikov, F. Orucevic, A.W. Rushforth, N. Welch, T.M. Benson, R.D. Wildman, T. Freegarde, M. Himsworth, J.

Ruostekoski, P. Smith, A. Tropper, P. F. Griffin, A. S. Arnold, E. Riis, J. E. Hastie, D. Paboeuf, D. C. Parrotta, B.M.Garraway, A.Pasquazi, M. Peccianti, W.Hensinger, E. Potter, A.H. Nizamani, H. Bostock, A. Rodriguez Blanco, G. Sinuco-León, I. R. Hill, R.A. Williams, P. Gill, N. Hempler, G. P. A. Malcolm, T. Cross, B. O. Kock, S. Maddox, P. John, "The UK National Quantum Technology Hub in Sensors and Metrology", SPIE Photonics Europe doi:10.1117/12.2232143 990009 (1-7) International Society for Optics and Photonics, May 2016 (2016).

[12] Nshii C.C., Vangeleyn M., Cotter J.P., Griffin P.F., Hinds E.A., Ironside C.N., See P., Sinclair A.G., Riis E. and Arnold A.S. A surface-patterned chip as a strong source of cold atoms for Quantum Technologies. *Nature Nanotechnology* 8 (2013), 321-324.

[13] Verhoeven J.C.J., Jansen J.K.M., Matheij R.M.M. and Smith W.R. Modelling laser-induced melting. *Mathematical and Computer Modelling* 37 (2003), 419-437.

[14] Cottrell A.H. and Hull D. Extrusion and Intrusion by Cyclic Slip in Copper *Proc. Royal Society A Mathematical, Physical and Engineering Sciences* 242(1229) (1957) 211-213.